

https://doi.org/10.3799/dqkx.2018.005



喜马拉雅造山带的部分熔融与淡色花岗岩成因机制

张泽明¹, 康东艳², 丁慧霞², 田作林¹, 董昕¹, 秦圣凯¹, 穆虹辰², 李梦梅²

1. 中国地质科学院地质研究所, 北京 100037

2. 中国地质大学地球科学与资源学院, 北京 100083

摘要: 喜马拉雅造山带核部由高级变质岩和淡色花岗岩组成, 是研究大陆碰撞造山带部分熔融与花岗岩成因的天然实验室。基于最新研究成果, 探讨了喜马拉雅造山带核部变质作用的条件、类型以及 $P-T$ 轨迹、部分熔融的方式与程度及熔体成分以及变质作用与部分熔融的时间和持续过程。相关证据表明, 造山带核部经历了高压麻粒岩相至榴辉岩相变质作用, 具有以增温增压进变质和近等温降压退变质为特征的顺时针型 $P-T$ 轨迹。这些高压变质岩石发生了长期持续的高温变质与部分熔融。在泥质岩石的进变质过程中白云母和黑云母脱水熔融可以形成不同成分的熔体。同时, 总结了淡色花岗岩的形成时间、地球化学特征和源区熔融方式, 结果表明碰撞造山过程中加厚下地壳的脱水熔融形成了喜马拉雅造山带的淡色花岗岩。

关键词: 高温与高压变质; 部分熔融; 时间和持续过程; 淡色花岗岩; 喜马拉雅造山带; 岩石学。

中图分类号: P581

文章编号: 1000-2383(2018)01-0082-17

收稿日期: 2017-09-23

Partial Melting of Himalayan Orogen and Formation Mechanism of Leucogranites

Zhang Zeming¹, Kang Dongyan², Ding Huixia², Tian Zuolin¹, Dong Xin¹, Qin Shengkai¹, Mu Hongchen², Li Mengmei²

1. Institute of Geology, Chinese Academy of Geological Sciences, Beijing 100037, China

2. School of Earth Sciences and Resources, China University of Geosciences, Beijing 100083, China

Abstract: The core of the Himalayan orogen consists of high-grade metamorphic rocks and leucogranites, forming a natural laboratory for studying crustal anatexis and granite origin during the collisional orogeny. Based on recent achievements of the related studies, the condition, type and $P-T$ path of metamorphism, and mechanism, degree and melt composition of anatexis as well as metamorphic and anatectic timing and duration of high-grade metamorphic rocks in the orogenic core are discussed in this paper. The obtained evidence shows that the orogenic core experienced high-pressure granulite-facies to eclogite-facies metamorphism, with a clockwise-type $P-T$ path characterized by increasing temperature and pressure prograde and early retrogression of near-isothermal decompression, and that the high-pressure rocks record a prolonged high-temperature metamorphic and anatectic process. The muscovite- and biotite-dehydration melting of meta-pelitic rocks during the prograde metamorphism resulted in formation of melts with highly variable chemical compositions. In addition, the formation time and geochemical feature of the Himalayan leucogranites are also summarized. Finally, it is concluded that the leucogranites were derived from the dehydration melting of thickened lower crust during the collisional orogeny.

Key words: high-temperature and high-pressure metamorphism; partial melting; time and duration; leucogranite; Himalayan orogen; petrology.

喜马拉雅造山带是印度和亚洲大陆在新生代碰撞作用的产物, 造山带核部由壮观的变质岩系和淡色花岗岩构成。由于这些岩石形成在一个单一的、已

知的造山作用过程中, 并没有叠加后期的构造热事件, 所以它们构成了一个研究碰撞造山过程中加厚下地壳岩石部分熔融与花岗岩成因的天然实验室。

基金项目: 国家科技重点研发项目(No.2016YFC060310); 国家自然科学基金项目(Nos.41230205, 41472056, 41602062)。

作者简介: 张泽明(1961—), 男, 研究员, 主要从事造山带变质作用与构造演化研究。ORCID: 0000-0002-6443-0718。

E-mail: zzm2111@sina.com; zmzhang181@163.com

引用格式: 张泽明, 康东艳, 丁慧霞, 等, 2018. 喜马拉雅造山带的部分熔融与淡色花岗岩成因机制. 地球科学, 43(1): 82-98.

近十几年来,关于喜马拉雅造山带变质与岩浆作用的研究取得了重要进展,为青藏高原的形成与演化提供了重要限定(Kohn, 2014; 吴福元等, 2015; 张泽明等, 2017).但是,有关造山带核部变质作用和部分熔融的条件、时间与持续过程、深熔机制、部分熔融程度与熔体成分,特别是部分熔融与淡色花岗岩的成因关系还存在不同认识.本文基于笔者自己的研究工作,结合现有研究成果,提出造山带核部普遍经历了高温和高压变质作用,各类岩石都经历了长期持续的高温变质与脱水熔融作用过程,形成了不同时代和成分复杂的淡色花岗岩.而且,提出大陆板块俯冲导致的地壳加厚与增温是引发深熔作用的主要构造机制,脱水熔融是部分熔融的主要方式.相关认识将为喜马拉雅造山带形成与演化模型的建立提供新的重要限定,同时也为古老造山带的相关研究提供借鉴.

1 地质背景

位于青藏高原南缘的喜马拉雅造山带是印度与亚洲大陆新生代碰撞作用的产物,是世界上最大且

仍在活动的碰撞造山带.喜马拉雅造山带呈弧形,从位于中国西藏的东构造结(Namche Barwa syntaxis,南迦巴瓦构造结)到巴基斯坦的西构造结(Nanga Parbat syntaxis,南迦帕尔巴特构造结)延伸长达 2 500 km(图 1).喜马拉雅造山带主要由 3 个构造单元组成,从北向南依次是,特提斯喜马拉雅岩系(Tethyan Himalayan sequence, THS)、高喜马拉雅岩系(Greater Himalayan sequence, GHS)和低喜马拉雅岩系(Lesser Himalayan sequence, LHS; Yin and Harrison, 2000).上述 3 个构造单元之间为藏南拆离系(South Tibetan detachment system, STD)和主中央逆冲断裂(Main central thrust, MCT).

高喜马拉雅系列主要由高级变质岩组成,而特提斯喜马拉雅系列和低喜马拉雅系列由中、低级变质岩和未变质的沉积岩组成.因此,这 3 个构造单元组成了一个夹心(三明治)构造,即高级变质的高喜马拉雅系列夹持在两个低级变质的构造单元之间.从低喜马拉雅系上部到高喜马拉雅系列下部,变质程度逐渐增高,即从低喜马拉雅系的绿泥石带、黑云母带、石榴石带到高喜马拉雅系列的十字石带、蓝晶石带和夕线石带,由此构成了世界上著名的反转变质带.特提斯喜马拉雅系列的最下部经历了低角闪

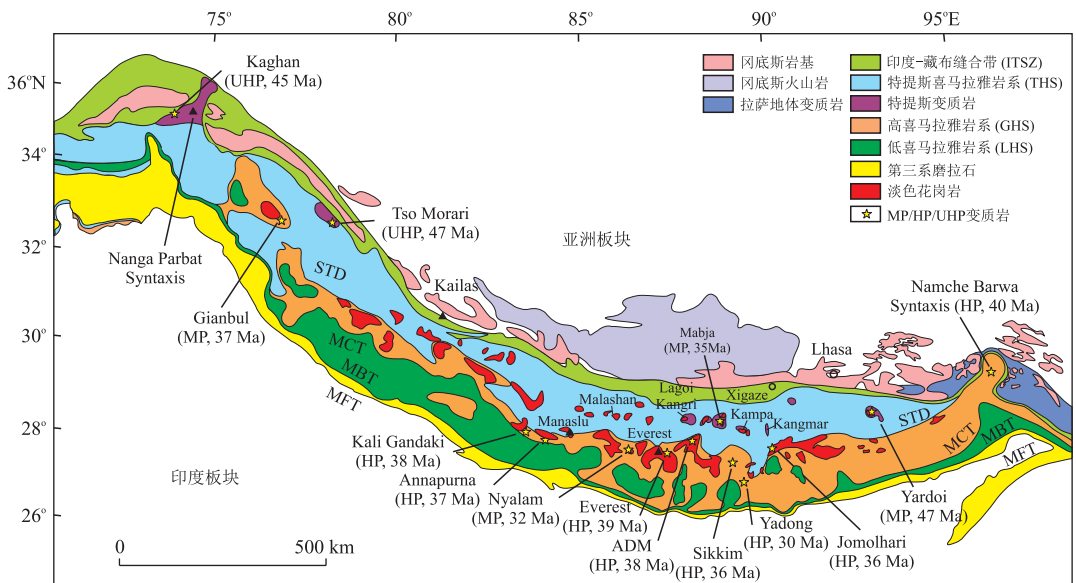


图 1 喜马拉雅造山带地质简图

Fig.1 Simplified geologic map of the Himalayan orogen

据 Yin and Harrison(2000)、Guillot *et al.*(2008)、Kohn(2014)、Ding *et al.*(2016a)修改;MFT,主前缘逆冲断裂;MBT,主边界逆冲断裂;MCT,主中央逆冲断裂;STD,藏南拆离系.图中标注了较深入研究的中、高级变质岩的地点与变质年龄,资料来源:ADM(Ama Drime Massif, Kellett *et al.*, 2014), Annapurna(Kohn and Corrie, 2011), Everest(Cottle *et al.*, 2009b), Gianbul(Horton *et al.*, 2015), Jomolhari(Regis *et al.*, 2014), Kaghan(Kaneko *et al.*, 2003), Kali Gandaki(Iaccarino *et al.*, 2015), Mabja dome(Lee and Whitehouse, 2007), Namche Barwa Syntaxis(Zhang *et al.*, 2015), Nyalam(Wang *et al.*, 2015a, 2015b), Sikkim(Rubatto *et al.*, 2013), Tso Moriri(Donaldson *et al.*, 2013), Yadong(Zhang *et al.*, 2017a)和 Yardoi dome(Ding *et al.*, 2016a, 2016b).变质作用类型:MP,中压;HP,高压;UHP,超高压

岩相变质作用,向上变质程度逐渐降低,直至未变质的沉积岩。由于上述 3 个构造单元之间的藏南拆离系和主中央逆冲断裂的位置存在争议,笔者在最近的研究中将喜马拉雅造山带核部的中、高级变质岩统称为喜马拉雅造山带变质核(Himalayan metamorphic core, HMC)。

在喜马拉雅造山带存在两条与造山带走向近平行产出的淡色花岗岩带,即沿高喜马拉雅岩系上部产出的高喜马拉雅淡色花岗岩带(Greater Himalayan leucogranite, GHL)和沿特提斯喜马拉雅岩系中部产出的特提斯喜马拉雅淡色花岗岩带(Tethyan Himalayan leucogranite, THL; 图 1; Le Fort, 1975, 1981; Guo and Wilson, 2012; 吴福元等, 2015)。在高喜马拉雅淡色花岗岩带,淡色花岗岩主要分布于高喜马拉雅岩系的上部构造层位,其产状各异,或者呈岩床状顺层侵入围岩,或者呈岩株状侵入,或呈较大的岩体。在特提斯喜马拉雅淡色花岗岩带,淡色花岗岩有两种产出形式,一种是位于特提斯喜马拉雅片麻岩穹窿核部,另一种以独立侵入体的形式侵入于特提斯喜马拉雅岩系之中(图 1)。

上述两条带中的淡色花岗岩具有类似的特征,主要由石英、钾长石、斜长石、黑云母、白云母、电气石和石榴石等组成,其中暗色矿物(黑云母)含量大多 $<5\%$,副矿物包括锆石、磷灰石、独居石、磷钇矿,有时有榍石、褐帘石、绿帘石和萤石。根据特征矿物的不同,这些岩石被划分为 3 大类型,即二云母花岗岩(包括黑云母花岗岩和白云母花岗岩)、电气石花岗岩和石榴石花岗岩(Scaillet *et al.*, 1990; Guillot and Le Fort, 1995)。少数地区还出现含红柱石、堇青石、夕线石和蓝晶石的淡色花岗岩(Daniel *et al.*, 2003; Streule *et al.*, 2010; Visonà *et al.*, 2012; Groppo *et al.*, 2013)。二云母花岗岩为喜马拉雅淡色花岗岩的主体岩石类型,而电气石花岗岩和石榴石花岗岩主要以规模不等的脉体赋存在二云母花岗岩中(吴福元等, 2015)。

2 高喜马拉雅岩系的变质条件与 $P-T$ 轨迹

在喜马拉雅造山带西段的 Tso Morari(印度西北部)和 Kaghan(巴基斯坦北部)地区,紧邻新特提斯洋缝合带产出有以含柯石英榴辉岩为代表的超高压变质岩(图 1; O'Brien *et al.*, 2001; Sachan *et*

al., 2004; St-Onge *et al.*, 2013)。这些岩石是印度大陆西北边缘快速陡俯冲到地幔深度经历超高压变质作用后又快速折返回上地壳的产物(Guillot *et al.*, 2008)。这些超高压变质岩具有 ~ 47 Ma 的峰期变质年龄和 ~ 40 Ma 的早期退变质年龄。有研究人员将这些岩石与分布于北喜马拉雅片麻岩穹窿中的变质岩一起称为特提斯变质岩(图 1; Guillot *et al.*, 2008)。

造山带核部的高喜马拉雅岩系是印度大陆平缓俯冲作用的产物,其具有与造山带北缘超高压变质岩完全不同的变质条件和时限。以前的研究大多表明,喜马拉雅造山带核部的高喜马拉雅岩系经历了典型的巴罗型中压变质作用。如在造山带中段锡金地区发育有典型的中压变质相系岩石,这里的反转变质带从下至上依次为黑云母带、石榴石带、十字石带、蓝晶石带、夕线石带和夕线石+钾长石带(Dasgupta *et al.*, 2004, 2009; Goscombe *et al.*, 2006; Rubatto *et al.*, 2013; Anczkiewicz *et al.*, 2014; Mottram *et al.*, 2014; Sorcar *et al.*, 2014; Gaidies *et al.*, 2015)。因此,中压型变质作用被认为是碰撞造山带变质作用的典型特征。但是,最近的研究表明,在造山带中东段的高喜马拉雅岩系普遍经历了高压麻粒岩相至榴辉岩相变质作用。泥质和长英质高压麻粒岩以石榴石+蓝晶石+黑云母+斜长石+钾长石+石英共生为特征,基性高压麻粒岩以石榴石+单斜辉石+斜长石+石英+金红石共生为特征。这些高压变质岩普遍叠加了中压麻粒岩相退变质作用,以夕线石、堇青石或斜方辉石等中-低压、高温矿物的出现为特征(Harris *et al.*, 2004; Imayama *et al.*, 2010, 2012; Guilmette *et al.*, 2011; Zhang *et al.*, 2015, 2017a)。造山带中段的 Ama Drime 地块经历了高压榴辉岩相变质作用,以麻粒岩化榴辉岩产出为特征(Lombardo and Rolfo, 2000; Groppo *et al.*, 2007; Guillot *et al.*, 2008; Cottle *et al.*, 2009a; Chakungal *et al.*, 2010; Corrie *et al.*, 2010; Grujic *et al.*, 2011; Warren *et al.*, 2011)。最新的研究确证了榴辉岩的存在(Wang *et al.*, 2017a)。

由于高压麻粒岩和榴辉岩经历了中、低压高温麻粒岩相退变质作用,导致被部分保留下来的峰期矿物化学成分发生变化;所以,用传统的地质温压计一般只会获得退变质作用期的温、压条件。这也正是造山带变质核被误以为仅经历了中压变质作用的重要原因。近年来的相平衡模拟研究揭示出,造山带核

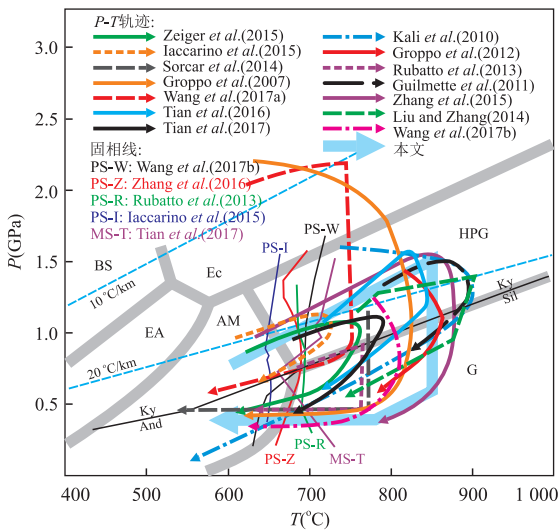


图 2 高喜马拉雅岩系变质作用 P - T 轨迹

Fig. 2 Metamorphic P - T paths of the Greater Himalayan sequence

变质相: AM.角闪岩相; BS.蓝片岩相; EA.绿帘角闪岩相; Ec.榴辉岩相; G.麻粒岩相; HPG.高压麻粒岩相; PS.泥质岩固相线; MS.基性岩固相线; 本文矿物代号: Am.角闪石; And.红柱石; Bt.黑云母; Cpx.单斜辉石; Crd.堇青石; Gt.石榴石; Kf.钾长石; Ilm.钛铁矿; Ky.蓝晶石; L.熔体; Ms.白云母; Pl.斜长石; Qz.石英; Rt.金红石; Sil.夕线石

部经历了高温、高压变质作用(图 2).在造山带东段的东喜马拉雅构造结,长英质麻粒岩的峰期变质条件为 1.5~1.6 GPa 和 850 °C (Guilmette *et al.*, 2011),或 1.5~1.6 GPa 和 825~835 °C (Tian *et al.*, 2016),泥质麻粒岩的峰期变质条件为 1.3~1.6 GPa 和 840~880 °C (Zhang *et al.*, 2015),基性麻粒岩的峰期变质条件为 1.4 GPa 和 904 °C (刘凤麟和张立飞, 2014)或 1.2 GPa 和 790 °C (田作林等, 2017);在造山带中段,尼泊尔 Ama Drime 地块含蓝晶石夕线石片麻岩的峰期变质条件 >1.4 GPa 和 >850 °C (Kali *et al.*, 2010).尼泊尔中部含蓝晶石片麻岩的峰变质条件为 >1.2 GPa 和 >800 °C (Groppo *et al.*, 2012),或为 1.0~1.1 GPa 和 710~720 °C (Iaccarino *et al.*, 2015).锡金地区含蓝晶石混合岩形成在 >1.0 GPa 的高压条件下 (Sorcar *et al.*, 2014).不丹地区含蓝晶石混合岩变质压力 >1.4 GPa (Regis *et al.*, 2014).在亚东地区,含蓝晶石夕线石片岩经历了 >1.2 GPa 和 >850 °C 的高温、高压麻粒岩相变质作用 (Zhang *et al.*, 2017a).对于造山带中段的麻粒岩化榴辉岩,其峰期压力 >1.5~2.0 GPa (Groppo *et al.*, 2007).新近, Wang *et al.* (2017a) 获得的榴辉岩峰期变质条件是 2.0~2.1 GPa 和 720~760 °C.因此,造山带核部的高级变

质岩很可能形成在 40~60 km 的加厚下地壳深度.

尽管近来的大多数研究表明,高喜马拉雅岩系记录了高压麻粒岩相至榴辉岩相峰期变质作用,但是,所获得的峰期变质条件差别较大(图 2).很可能有以下两方面原因:第一,由于后期高温退变质作用叠加,用相平衡模拟仍然无法获得岩石的真正峰期变质条件.许多研究只给出了岩石变质压力的下限,而不是最高压力;第二,不同地区,或者同一地区不同构造层位的变质岩具有不同的变质条件.如高压榴辉岩相变质的 Ama Drime 地块很可能是从更深的地壳中折返上来的,其与两侧的高喜马拉雅岩系之间为构造接触关系 (Cottle *et al.*, 2009a; Kali *et al.*, 2010; Kellett *et al.*, 2014).此外,近来的研究表明,高喜马拉雅岩系是由不同的构造岩片组成的,岩片之间存在明显的变质条件和(或)变质时间差异,即造山带核部存在变质-构造不连续现象 (Montomoli *et al.*, 2013, 2015; Larson and Cottle, 2014; Ambrose *et al.*, 2015; Larson *et al.*, 2015; Ding *et al.*, 2016a; 张泽明等, 2017).

尽管现有研究所给出的变质条件有较大不同,但是,所获得的 P - T 轨迹均为顺时针型(图 2),其进变质作用是以增温和增压为特征,反映印度大陆俯冲和地壳加厚过程;早期退变质作用是以近等温或者弱升温减压为特征,表明俯冲的印度大陆地壳发生了明显折返.部分研究还表明,高喜马拉雅岩系的晚期退变质作用是一个近等压的明显降温过程 (Groppo *et al.*, 2007; Rubatto *et al.*, 2013; Sorcar *et al.*, 2014; 图 2).这很可能表明,岩石折返到中上地壳以后有较长时间的停留,而并没有直接折返到地壳浅部.

3 高喜马拉雅岩系的部分熔融与熔体成分

观察表明,高喜马拉雅岩系中的各种岩石,包括基性、长英质和泥质变质岩都发生了部分熔融和混合岩化.但是,人们对高喜马拉雅岩系的熔融方式存在较大争议.以前的研究者普遍认为,高喜马拉雅岩系的部分熔融发生在减压退变质过程中,即近等温或升温过程中的减压导致了白云母和黑云母脱水熔融 (Pognante and Benna, 1993; Harris and Massey, 1994; Harris *et al.*, 1995, 2004; Harrison *et al.*, 1998; Patiño Douce and Harris, 1998; Searle,

1999; Zhang *et al.*, 2004; Aoya *et al.*, 2005; Viskupic *et al.*, 2005; King *et al.*, 2011). 得出这一结论的主要理由是, 岩石在最高压力下的变质温度低于含水矿物的脱水熔融温度, 但在降压过程中, 特别是在伴随有加热的降压过程中, 岩石的 P - T 轨迹要穿过具有正斜率的固相线, 由此导致脱水熔融. 但是, 这在很大程度上是由于以前的研究高估了白云母和黑云母的脱水熔融温度, 另一方面又低估了岩石在最高压力下的变质温度. 此外, 由于淡色花岗岩多在高喜马拉雅岩系顶部沿 STD 分布, 而且从大多淡色花岗岩中获得的锆石结晶年龄与 STD 的活动时间相似, 所以, 以前的研究者认为, STD 的活动导致了岩石的折返和降压, 诱发了岩石的部分熔融 (Cottle *et al.*, 2009a, 2009b).

但是, 就像图 2 和图 3 显示的, 最近的研究表明, 泥质和长英质岩石中白云母脱水熔融的温度在 $650 \sim 700 \text{ }^\circ\text{C}$ (Rubatto *et al.*, 2013; Iaccarino *et al.*, 2015; Zhang *et al.*, 2015; Wang *et al.*, 2017b), 变基性岩中角闪石的脱水熔融温度类似或略高 (田作林等, 2017). 尽管现有研究获得的高喜马拉雅岩系的变质温度有较大差别 ($720 \sim 900 \text{ }^\circ\text{C}$), 但这些岩石在最高压力下的变质温度都不同程度地超过了白云母脱水熔融温度 (图 2). 所以, 这些岩石在增温和增压的进变质过程中就可以发生部分熔融

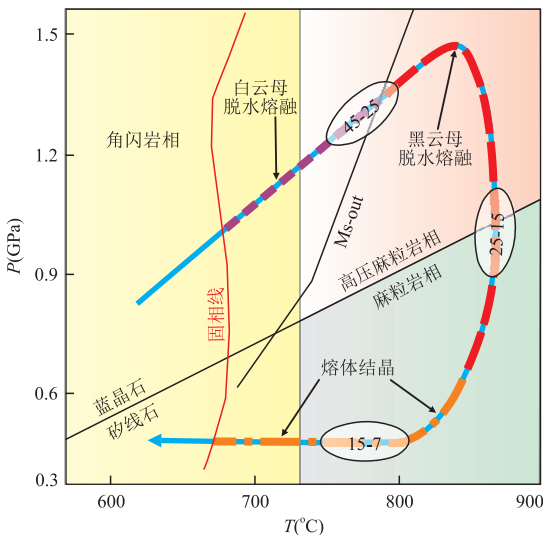


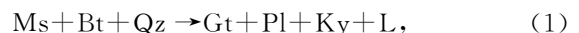
图 3 高喜马拉雅岩系的变质作用 P - T - t 轨迹以及白云母与黑云母脱水熔融和熔体结晶的时间与持续过程

Fig. 3 Metamorphic P - T - t path of the Greater Himalayan sequence, showing the timing and duration of muscovite- and biotite-dehydration, and melt crystallization

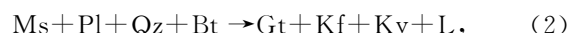
据 Gou *et al.* (2016)、张泽明等 (2017) 修改

(图 2 和图 3; Coleman, 1998; Godin *et al.*, 2001; Prince *et al.*, 2001; Viskupic and Hodges, 2001; Zhang *et al.*, 2004; Lee and Whitehouse, 2007; Cottle *et al.*, 2009a; Streule *et al.*, 2010; Guilmette *et al.*, 2011; Imayama *et al.*, 2012; Rubatto *et al.*, 2013; 向华等, 2013; Finch *et al.*, 2014; Regis *et al.*, 2014; Zhang *et al.*, 2015, 2017a, 2017b). Groppo *et al.* (2010, 2012) 研究揭示, 尼泊尔地区的长英质高压麻粒岩的部分熔融是发生在进变质到峰期 (蓝晶石稳定域) 变质过程中的白云母和黑云母脱水熔融, 熔融主要发生在加热条件下, 可以有也可以没有降压熔融的贡献. Rubatto *et al.* (2013) 认为, 锡金地区的泥质麻粒岩在进变质 (增温) 过程中先后发生了白云母和黑云母脱水熔融. Gou *et al.* (2016) 认为, 在印度大陆地壳俯冲过程中, 变泥质和长英质岩石经历了增温和增压进变质作用, 当变质温度达到 $\sim 650 \text{ }^\circ\text{C}$, 首先发生白云母脱水熔融, 再进一步增压增温 (达到峰压力) 和降压增温 (达到峰温度) 过程中发生黑云母脱水熔融 (图 3). 此外, 相关研究也表明, 高喜马拉雅岩系的部分熔融主要发生在高压变质条件下. 许多泥质和长英质混合岩的浅色体中含蓝晶石, 为加厚下地壳发生部分熔融提供了确切证据.

本文在 Zhang *et al.* (2017a) 对亚东地区高压泥质麻粒岩相平衡模拟基础上 (图 4a; 原文中样品 13-15, 图 10, 全岩化学成分为: $\text{SiO}_2 = 62.19\%$ 、 $\text{TiO}_2 = 0.78\%$ 、 $\text{Al}_2\text{O}_3 = 20.13\%$ 、 $\text{FeO} = 6.46\%$ 、 $\text{MnO} = 0.11\%$ 、 $\text{MgO} = 1.53\%$ 、 $\text{CaO} = 1.60\%$ 、 $\text{Na}_2\text{O} = 2.08\%$ 、 $\text{K}_2\text{O} = 3.41\%$ 、 $\text{H}_2\text{O} = 1.17\%$), 使用 Perple_X 程序计算了在增温 ($600 \sim 900 \text{ }^\circ\text{C}$) 和增压 ($0.7 \sim 1.6 \text{ GPa}$) 进变质过程中矿物和熔体体积, 以及熔体成分的变化 (图 4~6). 计算结果表明, 在部分熔融发生之前 (固相线以下), 随着进变质作用的进行, 黑云母和石英体积减小, 石榴石和斜长石体积增加 (图 4 和图 5), 表明发生黑云母脱水反应. 当部分熔融发生后, 随着熔融体积的逐渐增加, 白云母、黑云母和石英体积减小, 而石榴石、斜长石和蓝晶石体积增加, 相应的白云母 (+黑云母) 脱水熔融反应是:



在 1.38 GPa 和 $825 \text{ }^\circ\text{C}$ 左右的很窄区域内, 白云母快速消失, 斜长石也明显减少, 而钾长石快速生成, 熔体的体积明显增加, 相应的白云母脱水反应是:



当白云母消失后, 石英和黑云母快速减少, 而熔体和

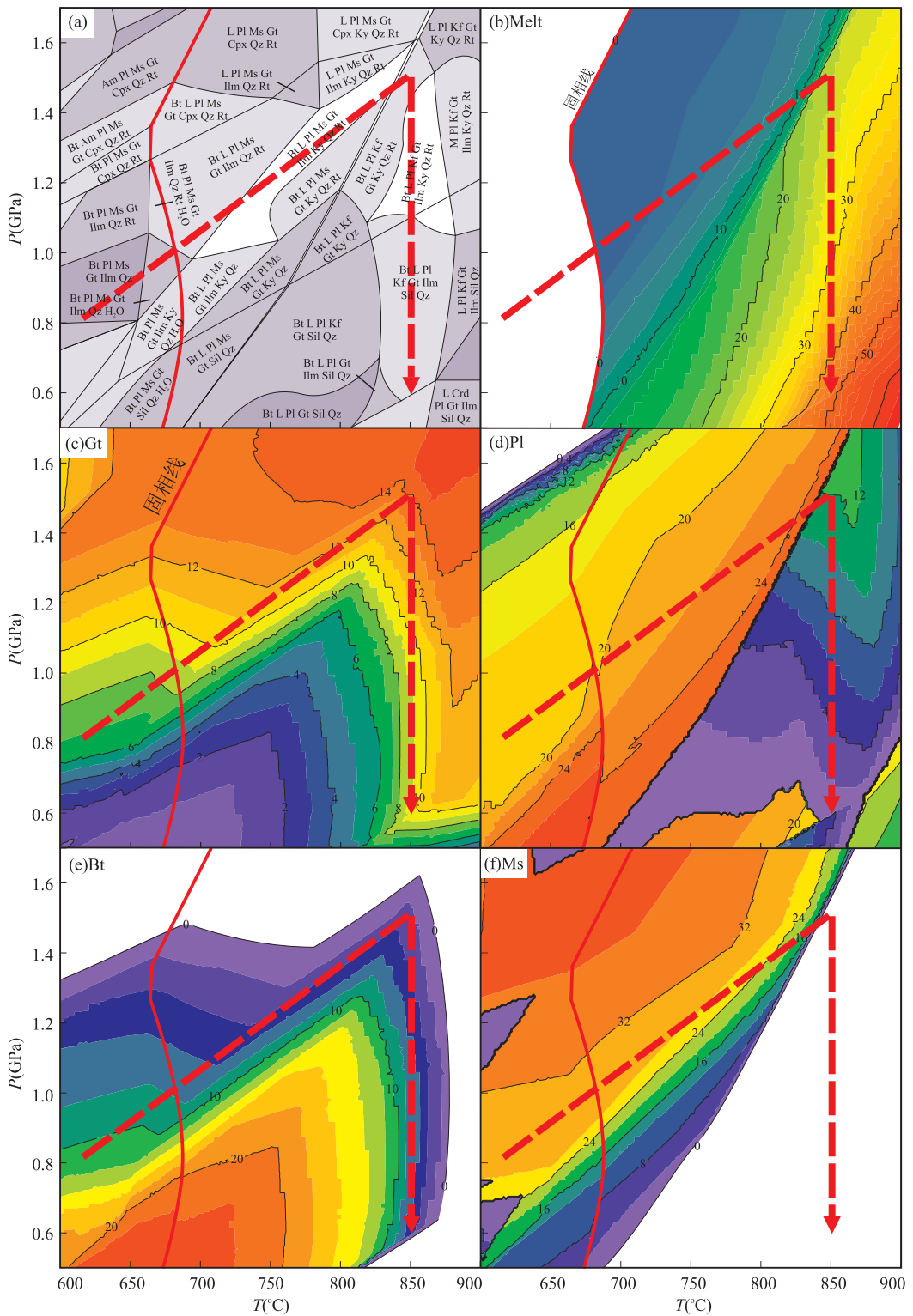
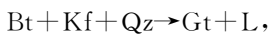


图 4 泥质麻粒岩的 $P-T$ 视剖图

Fig.4 $P-T$ pseudosections of the pelitic granulite

a. 矿物组合及稳定条件; b. 熔体体积; c~f. 分别为石榴石、斜长石、黑云母和白云母的体积。暖色代表含量高, 冷色代表含量低, 具体含量见图图中数字(%)

石榴石增加, 相应的黑云母脱水反应可能是:



(3)

在黑云母消失后的高温条件下, 相应的熔融反应可能是:

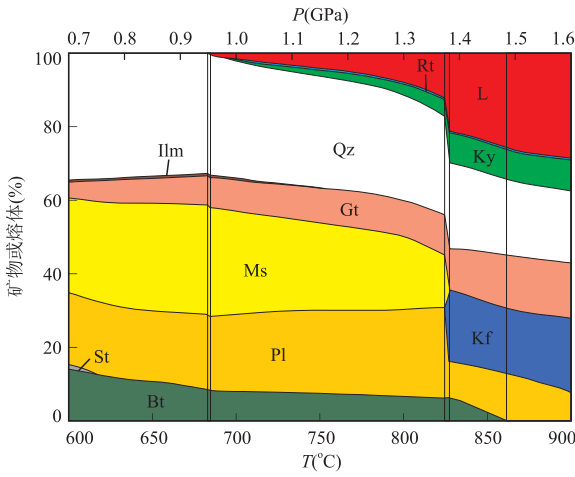


图 5 泥质麻粒岩进变质过程中矿物和熔体体积变化

Fig.5 Calculated changes of model proportions of minerals and melt during the increasing temperature (600–900 °C) and pressure (0.7–1.6 GPa) prograde metamorphism of the pelitic granulite



因此,总体来说,进变质过程中的部分熔融是以白云母和黑云母脱水熔融为主,但在白云母脱水熔融早期斜长石是生成物,而在晚期是反应物.石榴石、钾长石和蓝晶石总体上是生成物,即为转熔矿物.这与实际观察结果,以及这 3 个矿物中可含熔体包体是一致的.

计算结果表明,在近峰期变质条件下(1.4 GPa 和 850 °C),高压泥质麻粒岩发生了显著的部分熔融,熔体体积可达 20%~22%(图 4b 和图 5).在近等温降压退变质过程中,熔体的体积继续增加,甚至可能达到 30%~40%(图 4b).笔者计算出的进变质过程中所形成的熔体成分相当于花岗岩(6a),显示弱过铝质特征(图 6b),与高喜马拉雅淡色花岗岩成分类似(图 6).值得注意的是,熔体的化学成分变化较大(表 1,图 6).随着温度和压力增加,熔体的 SiO₂(74.58%~70.61%)和 Na₂O(6.70%~2.58%)含量逐渐减少,而 Al₂O₃(15.29%~16.38%)、FeO(0.33%~0.84%)、MgO(0.06%~0.15%),尤其是 CaO(0.41%~1.51%)和 K₂O(2.65%~7.92%)含量逐渐增加(表 1).初始熔体具有高的 SiO₂ 和 Na₂O 含量,低的 K₂O 含量,在 An-Ab-Or 图上落入奥长花岗岩区,随着熔融程度的增加,Na₂O 含量明显降低,而 K₂O 含量明显增加,进入花岗岩区(图 6d).

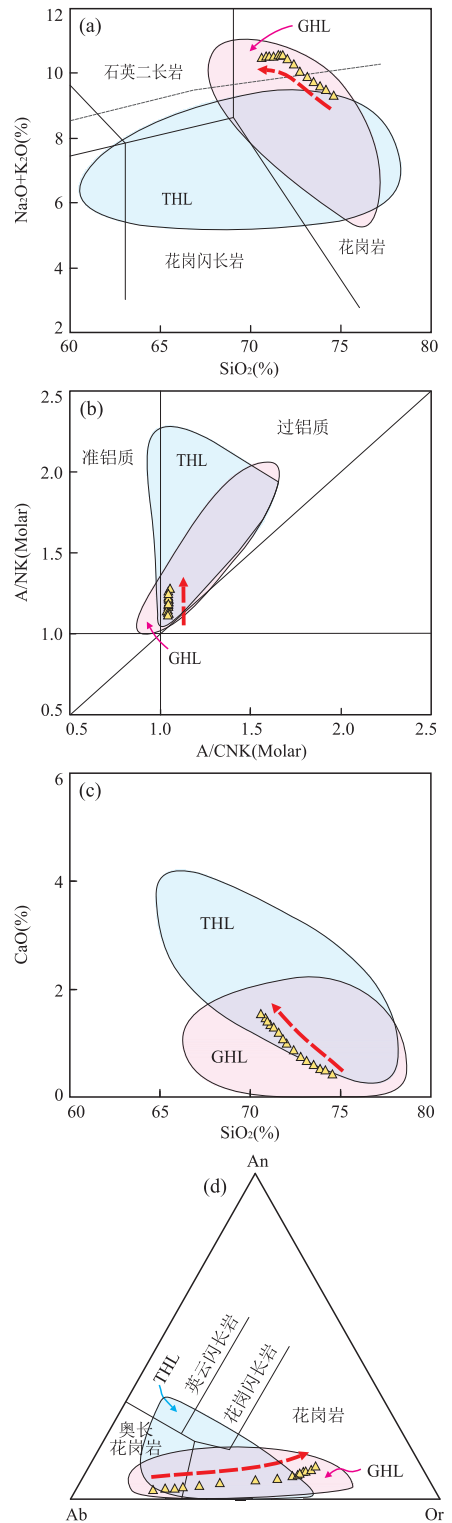


图 6 泥质麻粒岩进变质部分熔融过程中熔体成分变化

Fig.6 Calculated changes of melt compositions during the increasing temperature (600–900 °C) and pressure (0.7–1.6 GPa) prograde metamorphism of the pelitic granulite

图中箭头指示熔融程度增加.喜马拉雅淡色花岗岩的成分范围据吴福元等(2015).GHL.高喜马拉雅淡色花岗岩;THL.特提斯喜马拉雅淡色花岗岩

表 1 泥质麻粒岩进变质过程中所形成的熔体体积与成分计算结果

Table 1 Calculated mode and composition of melt of the pelitic granulites during the prograde metamorphism

| 计算条件 | P(GPa) | 1.00 | 1.05 | 1.10 | 1.15 | 1.20 | 1.25 | 1.30 | 1.35 | 1.38 | 1.39 | 1.40 | 1.45 | 1.50 | 1.55 | 1.60 |
|----------|--------------------------------|-------|-------|-------|-------|-------|-------|-------|-------|-------|-------|-------|-------|-------|-------|-------|
| | T(°C) | 700 | 717 | 733 | 750 | 767 | 783 | 800 | 817 | 833 | 850 | 867 | 883 | 900 | 825 | 828 |
| 熔体体积 | 体积含量(%) | 1.64 | 2.57 | 3.44 | 4.17 | 5.08 | 6.24 | 8.33 | 10.69 | 21.71 | 24.20 | 26.36 | 27.47 | 28.79 | 14.99 | 21.30 |
| | SiO ₂ | 74.58 | 74.17 | 73.88 | 73.49 | 73.12 | 72.76 | 72.37 | 72.02 | 71.76 | 71.63 | 71.53 | 71.32 | 71.05 | 70.84 | 70.61 |
| | Al ₂ O ₃ | 15.29 | 15.44 | 15.53 | 15.68 | 15.76 | 15.81 | 15.82 | 15.87 | 15.92 | 15.98 | 16.03 | 16.11 | 16.23 | 16.30 | 16.38 |
| | FeO | 0.33 | 0.37 | 0.41 | 0.45 | 0.50 | 0.55 | 0.57 | 0.60 | 0.60 | 0.58 | 0.59 | 0.65 | 0.69 | 0.76 | 0.84 |
| | MgO | 0.06 | 0.06 | 0.07 | 0.07 | 0.08 | 0.08 | 0.09 | 0.09 | 0.09 | 0.09 | 0.10 | 0.12 | 0.13 | 0.14 | 0.15 |
| 熔体成分 (%) | CaO | 0.41 | 0.46 | 0.51 | 0.56 | 0.64 | 0.73 | 0.85 | 0.96 | 1.06 | 1.14 | 1.17 | 1.26 | 1.35 | 1.43 | 1.51 |
| | Na ₂ O | 6.70 | 6.46 | 6.23 | 6.10 | 5.66 | 5.14 | 4.25 | 3.69 | 3.30 | 3.13 | 3.12 | 2.98 | 2.87 | 2.73 | 2.58 |
| | K ₂ O | 2.65 | 3.04 | 3.38 | 3.65 | 4.23 | 4.92 | 6.06 | 6.78 | 7.27 | 7.44 | 7.47 | 7.56 | 7.68 | 7.79 | 7.92 |
| | H ₂ O | 14.01 | 13.33 | 12.77 | 12.31 | 11.60 | 10.91 | 9.93 | 9.40 | 9.07 | 8.97 | 8.93 | 8.43 | 8.07 | 7.70 | 7.30 |
| | Or | 15.64 | 17.94 | 19.96 | 21.59 | 25.02 | 29.09 | 35.81 | 40.05 | 42.96 | 43.96 | 44.12 | 44.68 | 45.37 | 46.05 | 46.78 |
| | Ab | 56.67 | 54.70 | 52.74 | 51.57 | 47.90 | 43.46 | 35.92 | 31.22 | 27.90 | 26.46 | 26.37 | 25.24 | 24.24 | 23.08 | 21.87 |
| | An | 2.03 | 2.30 | 2.52 | 2.79 | 3.20 | 3.64 | 4.22 | 4.77 | 5.26 | 5.67 | 5.82 | 6.25 | 6.72 | 7.11 | 7.51 |

4 高喜马拉雅岩系部分熔融的时间与持续过程

喜马拉雅造山作用传统上被划分成两期,即中始新世到晚渐新世的始喜马拉雅期,对应于大陆碰撞、造山带地壳加厚和~33~28 Ma的峰期变质作用;早中新世至现今的新喜马拉雅期,对应于俯冲大陆地壳的折返,高温退变质作用、部分熔融和淡色花岗岩的侵入(Hodges, 2000; Jamieson *et al.*, 2004; Godin *et al.*, 2006).在造山带东段,从特提斯喜马拉雅变质穹隆中获得的最早期变质年龄为~47 Ma的锆石 U-Pb 年龄(Ding *et al.*, 2016a, 2016b)和 54~49 Ma 的石榴石 Lu-Hf 等值线年龄(Smit *et al.*, 2014).

大量的研究表明,利用锆石和独居石对高喜马拉雅岩系进行定年常常获得较大的年龄范围,如东喜马拉雅构造结的 43~7 Ma(Zhang *et al.*, 2010, 2012b, 2015),珠峰地区的 35~16 Ma(Imayama *et al.*, 2012)、聂拉木地区的 40~14 Ma(Wang *et al.*, 2013)、锡金地区的 36~17 Ma(Rubatto *et al.*, 2013)和尼泊尔地区的 42~16 Ma(Ambrose *et al.*, 2015).这表明高喜马拉雅岩系经历了长期持续的变质作用过程.对这些年龄的地质解释基本是一致的,大于 28~25 Ma 的年龄一般被认为是进变质年龄,较小的年龄被认为是退变质年龄.如在不丹中东部,高喜马拉雅岩系的进变质年龄为 36~28 Ma,退变质年龄为 28~13 Ma(Zeiger *et al.*, 2015).尼泊尔中部含蓝晶石片麻岩的进变质到峰期变质年龄为 43~28 Ma,退变质年龄为 25~18 Ma(Iaccarino *et al.*, 2015).聂拉木地区高喜马拉雅岩系的进变质年

龄为 35~20 Ma,退变质年龄在 20~15 Ma(Wang *et al.*, 2015a).

许多研究表明,高喜马拉雅岩系经历了~20 Ma 的持续高温变质与部分熔融过程(Cottle *et al.*, 2009a; Kellett *et al.*, 2013; Rubatto *et al.*, 2013; Wang *et al.*, 2013, 2016; Carosi *et al.*, 2014; Iaccarino *et al.*, 2015; Zhang *et al.*, 2015, 2017a).基于可获得的研究结果,张泽明等(2017)认为高喜马拉雅岩系的高温变质和部分熔融很可能在~45 Ma 就已经开始,并持续到~25 Ma 的峰期,之后是近等温降压退变质和可能的持续部分熔融.在~15~7 Ma,岩石经历了近等压降温退变质和熔体结晶过程(图 3).

事实上,前人在高喜马拉雅岩系混合岩浅色体和淡色花岗岩中已经获得了许多 35~25 Ma 的锆石结晶年龄(Coleman, 1998; Godin *et al.*, 2001; Prince *et al.*, 2001; Viskupic and Hodges, 2001; Zhang *et al.*, 2004; Lee and Whitehouse, 2007; Cottle *et al.*, 2009a; Groppo *et al.*, 2010; Imayama *et al.*, 2012; Rubatto *et al.*, 2013),甚至更早的锆石结晶年龄(~44 Ma; Aikman *et al.*, 2008, 2012; 戚学祥等, 2008; Zeng *et al.*, 2011; Gao *et al.*, 2012).这充分说明,高喜马拉雅岩系的部分熔融在 STD 开始活动(~25 Ma)之前就已经发生,并不像以往认为的那样,部分熔融发生在新喜马拉雅期,即高喜马拉雅岩系折返过程中的明显降压导致了部分熔融.

值得注意的是,部分研究显示,高喜马拉雅岩系内部的不同构造岩片的变质与熔融时间很可能是不同的.Kohn(2014)认为在尼泊尔中部,从上部向下部构造层位,变质与部分熔融的时间逐渐减小,其进

变质作用时间从最上部的~40~30 Ma 减小到最下部的 25~20 Ma, Wang *et al.* (2016) 也认为, 在尼泊尔地区高喜马拉雅岩系的上部构造岩片具有更早的变质与深熔年龄, 上部岩片的变质作用发生在 45~17 Ma, 部分熔融发生在~30~25 Ma, 而下部岩片的变质作用发生在 30~13 Ma, 部分熔融发生在~25~15 Ma. 但是, 也有研究者发现, 在尼泊尔地区, 高喜马拉雅岩系最下部构造层位的变质作用发生在 43~18 Ma, 部分熔融发生在 41~36 Ma (Carosi *et al.*, 2014) 或 36~28 Ma (Iaccarino *et al.*, 2015). 因此, 笔者认为高喜马拉雅岩系内部变质与深熔作用时间是否存在明显差异还需要深入研究. 现今, 笔者对定年矿物锆石和独居石的生长和分解行为仍然不是完全了解. 这些矿物的生长不仅受全岩成分、温度、压力和流体成分控制, 同时还取决于岩石的变质作用 P - T 轨迹 (Regis *et al.*, 2016). 有研究表明, 锆石和独居石在进变质和退变质过程中生长, 在部分熔融过程中分解 (Corrie and Kohn, 2011; Larson *et al.*, 2011; Tobgay *et al.*, 2012; Kohn, 2014; Regis *et al.*, 2016). 但也有研究表明, 锆石和独居石可以在部分熔融过程中结晶生长 (Rubatto *et al.*, 2013; Wang *et al.*, 2016).

5 对淡色花岗岩的成因制约

5.1 淡色花岗岩的形成时间

现今, 很多学者已经对喜马拉雅造山带的淡色花岗岩进行了定年研究, 大多定年结果表明它们形成在中新世 (25~10 Ma) (Guo and Wilson, 2012). 但是, 也陆续获得了一批较老的晚渐新世之前的年龄 (Ding *et al.*, 2005; Aikman *et al.*, 2008, 2012; 戚学祥等, 2008; Zeng *et al.*, 2011; Gao *et al.*, 2012; Hou *et al.*, 2012). 目前已知的淡色花岗岩形成时间在 46~7 Ma 之间, 其中特提斯喜马拉雅淡色花岗岩形成年龄较早, 在 46~8 Ma (Aoya *et al.*, 2005; Lee and Whitehouse, 2007; Aikman *et al.*, 2008, 2012; King *et al.*, 2011; Gao and Zeng, 2014; Liu *et al.*, 2014, 2016; 吴福元等, 2015), 而高喜马拉雅淡色花岗岩的形成相对较晚, 在 37~10 Ma 之间 (Guo and Wilson, 2012; Cottle *et al.*, 2015a). 吴福元等 (2015) 将淡色花岗岩的形成时间划分为始喜马拉雅 (44~26 Ma)、新喜马拉雅 (26~13 Ma) 和后喜马拉雅 (13~7 Ma) 3 个阶段.

事实上, 对单个淡色花岗岩样品中的锆石和独

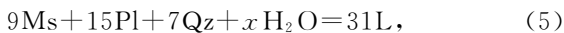
居石进行定年, 常常会获得很大的年龄范围, 或几组不同的年龄 (Lee and Whitehouse, 2007; Cottle *et al.*, 2007, 2009b; Langille *et al.*, 2012; Zeng *et al.*, 2012; Zhang *et al.*, 2012a; Lederer *et al.*, 2013). 对此可以有两种不同的解释, 一种是这些可变的年龄表明岩浆是通过多阶段部分熔融形成的, 另一种是岩浆经历了长时间持续结晶过程. 值得注意的是, 从具有岩浆结晶特征的锆石和独居石中获得的年龄仅代表它们的结晶年龄. 这个年龄可以等于或老于岩体的最后就位时间, 很可能晚于源区的部分熔融时间. 但是, 许多学者将这一结晶年龄直接推测为部分熔融时间, 由此得出高喜马拉雅岩系的部分熔融时间与 STD、MCT 的活动时间相同的结论 (Searle and Gondin, 2003; Streule *et al.*, 2010; Guo and Wilson, 2012; Cottle *et al.*, 2015b). 亚东地区混合岩化泥质麻粒岩的研究表明, 暗色体中的变质 (或深熔) 锆石给出了~30 Ma 的峰期变质和深熔年龄, 而原位和源区浅色体中岩浆结晶锆石给出的最小年龄为~13 Ma. 这表明从部分熔融晚期到最后熔体结晶之间可以有~20 Ma 的时间间隔 (张泽明等, 2017a). 笔者认为, 在高喜马拉雅岩系的长期持续熔融过程中, 如果所形成的熔体分批次抽离, 并快速上升就位, 就会形成不同时代的淡色花岗岩, 岩石中的锆石或独居石会给出较一致的结晶年龄. 如果所形成的熔体较长时间保留在源区, 或慢速上升, 所形成的淡色花岗岩中的锆石或独居石会获得可变的结晶年龄. 正如上文描述的, 变质岩石学和岩石年代学研究结果表明, 高喜马拉雅岩系经历了长期持续的部分熔融过程 (45~15 Ma), 这为形成具有不同锆石或独居石结晶年龄的淡色花岗岩提供了可能.

5.2 部分熔融方式

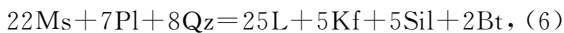
尽管喜马拉雅造山带的淡色花岗岩具有不同的产状、形成年龄和化学成分, 但是大家普遍认为它们是高喜马拉雅岩系部分熔融的产物, 而且多认为是泥质和长英质岩石发生深熔作用所致 (Harris and Massey, 1994; Patiño Douce and Harris, 1998; Zeng *et al.*, 2011, 2012; Guo and Wilson, 2012; Gao *et al.*, 2016; Gou *et al.*, 2016; Weinberg, 2016). 但是, 前人对高喜马拉雅岩系的熔融方式存在 3 种不同的认识, 即白云母和黑云母脱水熔融 (Harris *et al.*, 1993; Ganguly *et al.*, 2000; Dasgupta *et al.*, 2009; Kellett *et al.*, 2009; Groppo *et al.*, 2010, 2012, 2013; Streule *et al.*, 2010; Imayama *et al.*, 2012; Visonà *et al.*, 2012; Rubatto

et al., 2013; Gaidies *et al.*, 2015), 水致熔融 (water-fluxed melting, water-present melting or wet melting; Scaillet *et al.*, 1990; Prince *et al.*, 2001; Sachan *et al.*, 2010; King *et al.*, 2011; Guo and Wilson, 2012; Finch *et al.*, 2014; Gao and Zeng, 2014; Zeng *et al.*, 2015; 曾令森和高利娥, 2017) 或脱水熔融 + 水致熔融 (Pognante and Lombardo, 1989; Finch *et al.*, 2014).

有关水致熔融的观点主要来源于淡色花岗岩的地球化学研究。在喜马拉雅造山带, 有一部分淡色花岗岩具有高的 Sr 和 Ba 含量, 低的 Rb 含量和 $^{87}\text{Sr}/^{86}\text{Sr}(t)$ 比值, 而另外一部分具有较低的 Sr 和 Ba 含量、高的 Rb 含量和 $^{87}\text{Sr}/^{86}\text{Sr}(t)$ 比值。很多研究表明, 前一种淡色花岗岩是泥质岩石水致白云母熔融的产物, 而后一种是泥质岩中白云母脱水熔融的产物 (Gao and Zeng, 2014; Gao *et al.*, 2017; 曾令森和高利娥, 2017)。相关研究者认为水致白云母熔融的常见反应是:

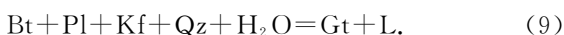


而白云母脱水熔融的常见反应是:



所以, 相对于白云母脱水熔融来说, 水致白云母熔融需要更多斜长石参与反应, 所形成的熔体具有更高的 Sr 和 Ba 含量, 低的 Rb 含量和 $^{87}\text{Sr}/^{86}\text{Sr}(t)$ 比值。

但是, 上述两个反应不足以全面描述高喜马拉雅岩系的熔融特征, 包括如下 4 方面内容: 第一, 高喜马拉雅岩系主要由正片麻岩、副片麻岩、斜长角闪岩和少量泥质岩组成, 这些岩石都不同程度地发生了部分熔融, 上述两个反应只适用于泥质石, 而不适用于其他岩石。第二, 大量淡色花岗岩含岩浆结晶的石榴石、黑云母或堇青石, 表明在部分熔融过程中必然有黑云母和角闪石参与, 而上述两个反应仅考虑了白云母熔融。第三, 泥质岩石的脱水熔融也非常复杂, 不能用上述反应 (6) 来概括。从上文的反应 (1) 中可以看出, 在白云母脱水熔融的早期阶段并没有斜长石参与, 从反应 (2) 中可以看出, 在白云母脱水熔融的晚期有大量的斜长石参与。而且, 在更高温条件下, 泥质岩的熔融表现为黑云母脱水熔融 (反应 (3))。第四, 即使是水致熔融, 也还存在如下可能的反应:



水致白云母熔融还有一个很重要的问题是水的来源, 无论在大陆地壳俯冲过程中, 还是在高压变质

岩折返过程中, 都不可能外来的大量水加入。而且, 即使是在岩石折返过程中有外来水加入, 还需要岩石保持较高的变质温度, 否则也不能发生水致熔融。因此, 正如上文描述的, 变质岩石学研究和相平衡模拟表明, 高喜马拉雅岩系进变质到早期退变质过程中的脱水熔融更可能是形成淡色花岗岩的主要熔融方式。

5.3 淡色花岗岩的地球化学成分

现有研究表明, 喜马拉雅造山带的淡色花岗岩具有高度变化的地球化学成分 (图 6)。有研究者认为这种成分变化是熔融方式不同或分离结晶作用所致, 也有研究者认为是源岩成分不同造成的。最近的研究大多表明, 高喜马拉雅岩系的长英质和泥质岩石, 包括基性岩 (King *et al.*, 2007; Zeng *et al.*, 2011; Hou *et al.*, 2012; Liu *et al.*, 2014), 都发生了脱水熔融。笔者相信, 源岩类型的不同, 同种原岩的成分差异以及部分熔融程度的不同是导致淡色花岗岩化学成分变化的主要原因。已有研究揭示, 变质基性岩的部分熔融可以形成高 Na/K 和 Sr/Y 值的淡色花岗岩 (King *et al.*, 2007; Zeng *et al.*, 2011; Hou *et al.*, 2012; Liu *et al.*, 2014)。更早期的研究表明, 淡色花岗岩的双峰式同位素成分特征表明它们起源于两个不同的源区, 具有较低 $^{87}\text{Sr}/^{86}\text{Sr}$ 初始比值的二云母淡色花岗岩是变质杂砂岩部分熔融的产物, 而具高 $^{87}\text{Sr}/^{86}\text{Sr}$ 初始比值的淡色花岗岩是泥质岩部分熔融的产物 (Guillot and Le Fort, 1995)。本研究揭示, 仅泥质岩石不同程度的脱水熔融就可以形成成分高度变化的熔体 (表 1; 图 6)。这和基性岩部分熔融的熔体成分在很大程度上取决于熔融程度的观点 (魏春景等, 2017) 是一致的。此外, 必然发生的熔体混合与同化混染, 以及残留和转熔矿物的存在, 都会使淡色花岗岩的化学成分发生复杂的变化, 而这些因素在以前的淡色花岗岩成因研究中未被充分考虑。

6 结论

(1) 喜马拉雅造山带核部经历了高压麻粒岩相至榴辉岩相变质作用, 并具有顺时针型的变质作用 P - T 轨迹, 其进变质以增温增压为特征, 退变质早期为近等温降压过程。但目前所获得的变质条件差别较大, 其中, 压力为 1.1~2.2 GPa, 温度为 750~900 °C。这或许表明造山带核部由不同的构造岩片组成, 或许是部分研究并没有获得岩石的实际

变质条件。

(2)高喜马拉雅岩系经历了强烈的白云母和黑云母脱水熔融,部分熔融主要发生在进变质和早期退变质过程中,所形成的熔体具有明显不同的化学成分。

(3)造山带核部经历了长期持续的高温变质、部分熔融和熔体结晶过程,深熔作用很可能在~45 Ma就已经开始,并持续到~15 Ma。

(4)大陆碰撞造山过程中加厚下地壳长期持续的脱水熔融可以形成广泛分布的、不同时代的和不同成分的淡色花岗岩。

致谢:谨以此文纪念我国著名岩石学家董申保院士为我国变质地质学发展做出的卓越贡献!感谢许志琴、金振民、莫宣学、吴福元和侯增谦院士,曾令森研究员,魏春景、赵志丹和朱弟成教授在工作中的指导与帮助!感谢周汉文教授和另一个审稿人提出的重要修改意见!

References

- Aikman, A. B., Harrison, T. M., Hermann, J., 2012. The Origin of Eo- and Neo-Himalayan Granitoids, Eastern Tibet. *Journal of Asian Earth Sciences*, 58: 143 – 157. <https://doi.org/10.1016/j.jseae.2012.05.018>
- Aikman, A. B., Harrison, T. M., Lin, D., 2008. Evidence for Early (> 44 Ma) Himalayan Crustal Thickening, Tethyan Himalaya, Southeastern Tibet. *Earth and Planetary Science Letters*, 274(1–2): 14–23. <https://doi.org/10.1016/j.epsl.2008.06.038>
- Ambrose, T. K., Larson, K. P., Guilmette, C., et al., 2015. Lateral Extrusion, Underplating, and Out-of-Sequence Thrusting within the Himalayan Metamorphic Core, Kanchenjunga, Nepal. *Lithosphere*, 7(4): 441 – 464. <https://doi.org/10.1130/l437.1>
- Anczkiewicz, R., Chakraborty, S., Dasgupta, S., et al., 2014. Timing, Duration and Inversion of Prograde Barrovian Metamorphism Constrained by High Resolution Lu-Hf Garnet Dating: A Case Study from the Sikkim Himalaya, NE India. *Earth and Planetary Science Letters*, 407: 70–81. <https://doi.org/10.1016/j.epsl.2014.09.035>
- Aoya, M., Wallis, S. R., Terada, K., et al., 2005. North-South Extension in the Tibetan Crust Triggered by Granite Emplacement. *Geology*, 33(11): 853. <https://doi.org/10.1130/g21806.1>
- Carosi, R., Montomoli, C., Langone, A., et al., 2014. Eocene Partial Melting Recorded in Peritectic Garnets from Kyanite Gneiss, Greater Himalayan Sequence, Central Nepal. *Geological Society, London, Special Publications*, 412(1): 111–129. <https://doi.org/10.1144/sp412.1>
- Chakungal, J., Dostal, J., Grujic, D., et al., 2010. Provenance of the Greater Himalayan Sequence: Evidence from Mafic Granulites and Amphibolites in NW Bhutan. *Tectonophysics*, 480(1–4): 198–212. <https://doi.org/10.1016/j.tecto.2009.10.014>
- Coleman, M. E., 1998. U-Pb Constraints on Oligocene-Miocene Deformation and Anatexis within the Central Himalaya, Marsyandi Valley, Nepal. *American Journal of Science*, 298(7): 553–571. <https://doi.org/10.2475/ajs.298.7.553>
- Corrie, S. L., Kohn, M. J., 2011. Metamorphic History of the Central Himalaya, Annapurna Region, Nepal, and Implications for Tectonic Models. *Geological Society of America Bulletin*, 123(9–10): 1863–1879. <https://doi.org/10.1130/b30376.1>
- Corrie, S. L., Kohn, M. J., Vervoort, J. D., 2010. Young Eclogite from the Greater Himalayan Sequence, Arun Valley, Eastern Nepal: *P-T-t* Path and Tectonic Implications. *Earth and Planetary Science Letters*, 289(3–4): 406–416. <https://doi.org/10.1016/j.epsl.2009.11.029>
- Cottle, J. M., Jessup, M. J., Newell, D. L., et al., 2007. Structural Insights into the Early Stages of Exhumation along an Orogen-Scale Detachment: The South Tibetan Detachment System, Dzaka Chu Section, Eastern Himalaya. *Journal of Structural Geology*, 29(11): 1781–1797. <https://doi.org/10.1016/j.jsg.2007.08.007>
- Cottle, J. M., Jessup, M. J., Newell, D. L., et al., 2009a. Geochronology of Granulitized Eclogite from the Ama Drime Massif: Implications for the Tectonic Evolution of the South Tibetan Himalaya. *Tectonics*, 28(1): TC1002. <https://doi.org/10.1029/2008tc002256>
- Cottle, J. M., Larson, K. P., Kellett, D. A., 2015a. How does the Mid-Crust Accommodate Deformation in Large, Hot Collisional Orogens? A Review of Recent Research in the Himalayan Orogen. *Journal of Structural Geology*, 78: 119–133. <https://doi.org/10.1016/j.jsg.2015.06.008>
- Cottle, J. M., Searle, M. P., Horstwood, M. S. A., et al., 2009b. Timing of Midcrustal Metamorphism, Melting, and Deformation in the Mount Everest Region of Southern Tibet Revealed by U(-Th)-Pb Geochronology. *The Journal of Geology*, 117(6): 643–664. <https://doi.org/10.1086/605994>
- Cottle, J. M., Searle, M. P., Jessup, M. J., et al., 2015b. Rongbuk Re-Visited: Geochronology of Leucogranites in the Footwall of the South Tibetan Detachment System, Everest Region, Southern Tibet. *Lithos*, 227: 94–106.

- <https://doi.org/10.1016/j.lithos.2015.03.019>
- Daniel, C.G., Hollister, L.S., Parrish, R.R., et al., 2003. Exhumation of the Main Central Thrust from Lower Crustal Depths, Eastern Bhutan Himalaya. *Journal of Metamorphic Geology*, 21(4): 317–334. <https://doi.org/10.1046/j.1525-1314.2003.00445.x>
- Dasgupta, S., Chakraborty, S., Neogi, S., 2009. Petrology of an Inverted Barrovian Sequence of Metapelites in Sikkim Himalaya, India: Constraints on the Tectonics of Inversion. *American Journal of Science*, 309(1): 43–84. <https://doi.org/10.2475/01.2009.02>
- Dasgupta, S., Ganguly, J., Neogi, S., 2004. Inverted Metamorphic Sequence in the Sikkim Himalayas; Crystallization History, P - T Gradient and Implications. *Journal of Metamorphic Geology*, 22(5): 395–412. <https://doi.org/10.1111/j.1525-1314.2004.00522.x>
- Ding, H. X., Zhang, Z. M., Dong, X., et al., 2016a. Early Eocene (c.50 Ma) Collision of the Indian and Asian Continents; Constraints from the North Himalayan Metamorphic Rocks, Southeastern Tibet. *Earth and Planetary Science Letters*, 435: 64–73. <https://doi.org/10.1016/j.epsl.2015.12.006>
- Ding, H.X., Zhang, Z.M., Hu, K.M., et al., 2016b. P - T - t - D Paths of the North Himalayan Metamorphic Rocks; Implications for the Himalayan Orogeny. *Tectonophysics*, 683: 393–404. <https://doi.org/10.1016/j.tecto.2016.06.035>
- Ding, L., Kapp, P., Wan, X. Q., 2005. Paleocene-Eocene Record of Ophiolite Obduction and Initial India-Asia Collision, South Central Tibet. *Tectonics*, 24(3): TC3001. <https://doi.org/10.1029/2004tc001729>
- Donaldson, D.G., Webb, A. A. G., Menold, C. A., et al., 2013. Petrochronology of Himalayan Ultrahigh-Pressure Eclogite. *Geology*, 41(8): 835–838. <https://doi.org/10.1130/g33699.1>
- Finch, M., Hasalova, P., Weinberg, R. F., et al., 2014. Switch from Thrusting to Normal Shearing in the Zaskar Shear Zone, NW Himalaya: Implications for Channel Flow. *Geological Society of America Bulletin*, 126(7–8): 892–924. <https://doi.org/10.1130/b30817.1>
- Gaidies, F., Petley-Ragan, A., Chakraborty, S., et al., 2015. Constraining the Conditions of Barrovian Metamorphism in Sikkim, India: P - T Paths of Garnet Crystallization in the Lesser Himalayan Belt. *Journal of Metamorphic Geology*, 33(1): 23–44. <https://doi.org/10.1111/jmg.12108>
- Ganguly, J., Dasgupta, S., Cheng, W. J., et al., 2000. Exhumation History of a Section of the Sikkim Himalayas, India: Records in the Metamorphic Mineral Equilibria and Compositional Zoning of Garnet. *Earth and Planetary Science Letters*, 183(3–4): 471–486. [https://doi.org/10.1016/s0012-821x\(00\)00280-6](https://doi.org/10.1016/s0012-821x(00)00280-6)
- Gao, L. E., Zeng, L. S., 2014. Fluxed Melting of Metapelite and the Formation of Miocene High-CaO Two-Mica Granites in the Malashan Gneiss Dome, Southern Tibet. *Geochimica et Cosmochimica Acta*, 130: 136–155. <https://doi.org/10.1016/j.gca.2014.01.003>
- Gao, L. E., Zeng, L. S., Asimow, P. D., 2017. Contrasting Geochemical Signatures of Fluid-Absent versus Fluid-Fluxed Melting of Muscovite in Metasedimentary Sources: The Himalayan Leucogranites. *Geology*, 45(1): 39–42. <https://doi.org/10.1130/g38336.1>
- Gao, L. E., Zeng, L. S., Gao, J. H., et al., 2016. Oligocene Crustal Anatexis in the Tethyan Himalaya, Southern Tibet. *Lithos*, 264: 201–209. <https://doi.org/10.1016/j.lithos.2016.08.038>
- Gao, L. E., Zeng, L. S., Xie, K. J., 2012. Eocene High Grade Metamorphism and Crustal Anatexis in the North Himalaya Gneiss Domes, Southern Tibet. *Chinese Science Bulletin*, 57(6): 639–650. <https://doi.org/10.1007/s11434-011-4805-4>
- Godin, L., Grujic, D., Law, R. D., et al., 2006. Channel Flow, Ductile Extrusion and Exhumation in Continental Collision Zones: An Introduction. *Geological Society, London, Special Publications*, 268: 1–23.
- Godin, L., Parrish, R. R., Brown, R. L., et al., 2001. Crustal Thickening Leading to Exhumation of the Himalayan Metamorphic Core of Central Nepal: Insight from U-Pb Geochronology and $^{40}\text{Ar}/^{39}\text{Ar}$ Thermochronology. *Tectonics*, 20(5): 729–747. <https://doi.org/10.1029/2000tc001204>
- Goscombe, B., Gray, D., Hand, M., 2006. Crustal Architecture of the Himalayan Metamorphic Front in Eastern Nepal. *Gondwana Research*, 10(3–4): 232–255. <https://doi.org/10.1016/j.gr.2006.05.003>
- Gou, Z. B., Zhang, Z. M., Dong, X., et al., 2016. Petrogenesis and Tectonic Implications of the Yadong Leucogranites, Southern Himalaya. *Lithos*, 256–257: 300–310. <https://doi.org/10.1016/j.lithos.2016.04.009>
- Groppo, C., Lombardo, B., Rolfo, F., et al., 2007. Clockwise Exhumation Path of Granulitized Eclogites from the Ama Drime Range (Eastern Himalayas). *Journal of Metamorphic Geology*, 25(1): 51–75. <https://doi.org/10.1111/j.1525-1314.2006.00678.x>
- Groppo, C., Rolfo, F., Indares, A., 2012. Partial Melting in the Higher Himalayan Crystallines of Eastern Nepal: The Effect of Decompression and Implications for the Channel

- Flow Model. *Journal of Petrology*, 53 (5): 1057 – 1058. <https://doi.org/10.1093/petrology/egs009>
- Groppo, C., Rolfo, F., Mosca, P., 2013. The Cordierite-Bearing Anatexitic Rocks of the Higher Himalayan Crystallines (Eastern Nepal): Low-Pressure Anatexis, Melt Productivity, Melt Loss and the Preservation of Cordierite. *Journal of Metamorphic Geology*, 31 (2): 187 – 204. <https://doi.org/10.1111/jmg.12014>
- Groppo, C., Rubatto, D., Rolfo, F., et al., 2010. Early Oligocene Partial Melting in the Main Central Thrust Zone (Arun Valley, Eastern Nepal Himalaya). *Lithos*, 118 (3 – 4): 287 – 301. <https://doi.org/10.1016/j.lithos.2010.05.003>
- Grujic, D., Warren, C. J., Wooden, J. L., 2011. Rapid Synconvergent Exhumation of Miocene-Aged Lower Orogenic Crust in the Eastern Himalaya. *Lithosphere*, 3 (5): 346 – 366. <https://doi.org/10.1130/1154.1>
- Guillot, S., Le Fort, P., 1995. Geochemical Constraints on the Bimodal Origin of High Himalayan Leucogranites. *Lithos*, 35 (3 – 4): 221 – 234. [https://doi.org/10.1016/0024-4937\(94\)00052-4](https://doi.org/10.1016/0024-4937(94)00052-4)
- Guillot, S., Mahéo, G., de Sigoyer, J., et al., 2008. Tethyan and Indian Subduction Viewed from the Himalayan High-to Ultrahigh-Pressure Metamorphic Rocks. *Tectonophysics*, 451 (1 – 4): 225 – 241. <https://doi.org/10.1016/j.tecto.2007.11.059>
- Guilmette, C., Indares, A., Hébert, R., 2011. High-Pressure Anatexitic Paragneisses from the Namche Barwa, Eastern Himalayan Syntaxis: Textural Evidence for Partial Melting, Phase Equilibria Modeling and Tectonic Implications. *Lithos*, 124 (1 – 2): 66 – 81. <https://doi.org/10.1016/j.lithos.2010.09.003>
- Guo, Z. F., Wilson, M., 2012. The Himalayan Leucogranites: Constraints on the Nature of Their Crustal Source Region and Geodynamic Setting. *Gondwana Research*, 22 (2): 360 – 376. <https://doi.org/10.1016/j.gr.2011.07.027>
- Harris, N. B. W., Ayres, M. W., Massey, J. A., 1995. Geochemistry of Granitic Melts Produced during the Incongruent Melting of Muscovite: Implications for the Extraction of Himalayan Leucogranite Magmas. *Journal of Geophysical Research: Solid Earth*, 100 (B8): 15767 – 15777. <https://doi.org/10.1029/94jb02623>
- Harris, N. B. W., Caddick, M., Kosler, J., et al., 2004. The Pressure-Temperature-Time Path of Migmatites from the Sikkim Himalaya. *Journal of Metamorphic Geology*, 22 (3): 249 – 264. <https://doi.org/10.1111/j.1525-1314.2004.00511.x>
- Harris, N. B. W., Inger, S., Massey, J., 1993. The Role of Fluids in the Formation of High Himalayan Leucogranites. *Geological Society, London, Special Publications*, 74: 391 – 400.
- Harris, N. B. W., Massey, J. A., 1994. Decompression and Anatexis of Himalayan Metapelites. *Tectonics*, 13 (6): 1537 – 1546. <https://doi.org/10.1029/94tc01611>
- Harrison, T. M., Grove, M., Lovera, O. M., et al., 1998. A Model for the Origin of Himalayan Anatexis and Inverted Metamorphism. *Journal of Geophysical Research: Solid Earth*, 103 (B11): 27017 – 27032. <https://doi.org/10.1029/98jb02468>
- Hodges, K. V., 2000. Tectonics of the Himalaya and Southern Tibet from Two Perspectives. *Geological Society of America Bulletin*, 112 (3): 324 – 350. [https://doi.org/10.1130/0016-7606\(2000\)112<324:tothas>2.0.co;2](https://doi.org/10.1130/0016-7606(2000)112<324:tothas>2.0.co;2)
- Horton, F., Lee, J., Hacker, B., et al., 2015. Himalayan Gneiss Dome Formation in the Middle Crust and Exhumation by Normal Faulting: New Geochronology of Gianbul Dome, Northwestern India. *Geological Society of America Bulletin*, 127 (1 – 2): 162 – 180. <https://doi.org/10.1130/b31005.1>
- Hou, Z. Q., Zheng, Y. C., Zeng, L. S., et al., 2012. Eocene-Oligocene Granitoids in Southern Tibet: Constraints on Crustal Anatexis and Tectonic Evolution of the Himalayan Orogen. *Earth and Planetary Science Letters*, 349 – 350: 38 – 52. <https://doi.org/10.1016/j.epsl.2012.06.030>
- Iaccarino, S., Montomoli, C., Carosi, R., et al., 2015. Pressure-Temperature-Time-Deformation Path of Kyanite-Bearing Migmatitic Paragneiss in the Kali Gandaki Valley (Central Nepal): Investigation of Late Eocene-Early Oligocene Melting Processes. *Lithos*, 231: 103 – 121. <https://doi.org/10.1016/j.lithos.2015.06.005>
- Imayama, T., Takeshita, T., Arita, K., 2010. Metamorphic *P-T* Profile and *P-T* Path Discontinuity across the Far-Eastern Nepal Himalaya: Investigation of Channel Flow Models. *Journal of Metamorphic Geology*, 28 (5): 527 – 549. <https://doi.org/10.1111/j.1525-1314.2010.00879.x>
- Imayama, T., Takeshita, T., Yi, K., et al., 2012. Two-Stage Partial Melting and Contrasting Cooling History within the Higher Himalayan Crystalline Sequence in the Far-Eastern Nepal Himalaya. *Lithos*, 134 – 135: 1 – 22. <https://doi.org/10.1016/j.lithos.2011.12.004>
- Jamieson, R. A., Beaumont, C., Medvedev, S., et al., 2004. Crustal Channel Flows: 2. Numerical Models with Implications for Metamorphism in the Himalayan-Tibetan Orogen. *Journal of Geophysical Research: Solid Earth*, 109 (B6): B06407. <https://doi.org/10.1029/2003jb002811>
- Kali, E., Leloup, P. H., Arnaud, N., et al., 2010. Exhumation

- History of the Deepest Central Himalayan Rocks, Ama Drime Range; Key Pressure-Temperature-Deformation-Time Constraints on Orogenic Models. *Tectonics*, 29 (2): TC2014. <https://doi.org/10.1029/2009TC002551>
- Kaneko, Y., Katayama, I., Yamamoto, H., et al., 2003. Timing of Himalayan Ultrahigh-Pressure Metamorphism; Sinking Rate and Subduction Angle of the Indian Continental Crust beneath Asia. *Journal of Metamorphic Geology*, 21 (6): 589 – 599. <https://doi.org/10.1046/j.1525-1314.2003.00466.x>
- Kellett, D. A., Cottle, J. M., Smit, M., 2014. Eocene Deep Crust at Ama Drime, Tibet: Early Evolution of the Himalayan Orogen. *Lithosphere*, 6 (4): 220 – 229. <https://doi.org/10.1130/1350.1>
- Kellett, D. A., Grujic, D., Coutand, I., et al., 2013. The South Tibetan Detachment System Facilitates Ultra Rapid Cooling of Granulite-Facies Rocks in Sikkim Himalaya. *Tectonics*, 32 (2): 252 – 270. <https://doi.org/10.1002/tect.20014>
- Kellett, D. A., Grujic, D., Erdmann, S., 2009. Miocene Structural Reorganization of the South Tibetan Detachment, Eastern Himalaya; Implications for Continental Collision. *Lithosphere*, 1 (5): 259 – 281. <https://doi.org/10.1130/156.1>
- King, J., Harris, N., Argles, T., et al., 2007. First Field Evidence of Southward Ductile Flow of Asian Crust beneath Southern Tibet. *Geology*, 35 (8): 727. <https://doi.org/10.1130/g23630a.1>
- King, J., Harris, N., Argles, T., et al., 2011. Contribution of Crustal Anatexis to the Tectonic Evolution of Indian Crust beneath Southern Tibet. *Geological Society of America Bulletin*, 123 (1 – 2): 218 – 239. <https://doi.org/10.1130/b30085.1>
- Kohn, M. J., 2014. Himalayan Metamorphism and Its Tectonic Implications. *Annual Review of Earth and Planetary Sciences*, 42 (1): 381 – 419. <https://doi.org/10.1146/annurev-earth-060313-055005>
- Kohn, M. J., Corrie, S. L., 2011. Preserved Zr-Temperatures and U-Pb Ages in High-Grade Metamorphic Titanite; Evidence for a Static Hot Channel in the Himalayan Orogen. *Earth and Planetary Science Letters*, 311 (1 – 2): 136 – 143. <https://doi.org/10.1016/j.epsl.2011.09.008>
- Langille, J. M., Jessup, M. J., Cottle, J. M., et al., 2012. Timing of Metamorphism, Melting and Exhumation of the Leo Pargil Dome, Northwest India. *Journal of Metamorphic Geology*, 30 (8): 769 – 791. <https://doi.org/10.1111/j.1525-1314.2012.00998.x>
- Larson, K. P., Ambrose, T. K., Webb, A. A. G., et al., 2015. Reconciling Himalayan Midcrustal Discontinuities; The Main Central Thrust System. *Earth and Planetary Science Letters*, 429: 139 – 146. <https://doi.org/10.1016/j.epsl.2015.07.070>
- Larson, K. P., Cottle, J. M., 2014. Midcrustal Discontinuities and the Assembly of the Himalayan Midcrust. *Tectonics*, 33 (5): 718 – 740. <https://doi.org/10.1002/2013tc003452>
- Larson, K. P., Cottle, J. M., Godin, L., 2011. Petrochronologic Record of Metamorphism and Melting in the Upper Greater Himalayan Sequence, Manaslu-Himal Chuli Himalaya, West-Central Nepal. *Lithosphere*, 3 (6): 379 – 392. <https://doi.org/10.1130/1149.1>
- Le Fort, P., 1975. Himalayas: The Collided Range. Present Knowledge of the Continental Arc. *American Journal of Science*, 275: 1 – 44.
- Le Fort, P., 1981. Manaslu Leucogranite; A Collision Signature of the Himalaya; A Model for Its Genesis and Emplacement. *Journal of Geophysical Research: Solid Earth*, 86 (B11): 10545 – 10568. <https://doi.org/10.1029/jb086ib11p10545>
- Lederer, G. W., Cottle, J. M., Jessup, M. J., et al., 2013. Timescales of Partial Melting in the Himalayan Middle Crust; Insight from the Leo Pargil Dome, Northwest India. *Contributions to Mineralogy and Petrology*, 166 (5): 1415 – 1441. <https://doi.org/10.1007/s00410-013-0935-9>
- Lee, J., Whitehouse, M. J., 2007. Onset of Mid-Crustal Extensional Flow in Southern Tibet; Evidence from U/Pb Zircon Ages. *Geology*, 35 (1): 45. <https://doi.org/10.1130/g22842a.1>
- Liu, F. L., Zhang, L. F., 2014. High-Pressure Granulites from Eastern Himalayan Syntaxis; P-T Path, Zircon U-Pb Dating and Geological Implications. *Acta Petrologica Sinica*, 30 (10): 2808 – 2820 (in Chinese with English abstract).
- Liu, Z. C., Wu, F. Y., Ding, L., et al., 2016. Highly Fractionated Late Eocene (~35 Ma) Leucogranite in the Xiaru Dome, Tethyan Himalaya, South Tibet. *Lithos*, 240 – 243: 337 – 354. <https://doi.org/10.1016/j.lithos.2015.11.026>
- Liu, Z. C., Wu, F. Y., Ji, W. Q., et al., 2014. Petrogenesis of the Ramba Leucogranite in the Tethyan Himalaya and Constraints on the Channel Flow Model. *Lithos*, 208 – 209: 118 – 136. <https://doi.org/10.1016/j.lithos.2014.08.022>
- Lombardo, B., Rolfo, F., 2000. Two Contrasting Eclogite Types in the Himalayas; Implications for the Himalayan Orogeny. *Journal of Geodynamics*, 30 (1 – 2): 37 – 60. [https://doi.org/10.1016/s0264-3707\(99\)00026-5](https://doi.org/10.1016/s0264-3707(99)00026-5)
- Montomoli, C., Carosi, R., Iaccarino, S., 2015. Tectonometamorphic Discontinuities in the Greater Himalayan Se-

- quence; A Local or a Regional Feature? *Geological Society, London, Special Publication*, 412 (1): 25–41. <https://doi.org/10.1144/SP412.3>
- Montomoli, C., Iaccarino, S., Carosi, R., et al., 2013. Tectono-metamorphic Discontinuities within the Greater Himalayan Sequence in Western Nepal (Central Himalaya): Insights on the Exhumation of Crystalline Rocks. *Tectonophysics*, 608: 1349–1370. <https://doi.org/10.1016/j.tecto.2013.06.006>
- Mottram, C. M., Warren, C. J., Regis, D., et al., 2014. Developing an Inverted Barrovian Sequence: Insights from Monazite Petrochronology. *Earth and Planetary Science Letters*, 403: 418–431. <https://doi.org/10.1016/j.epsl.2014.07.006>
- O'Brien, P. J., Zotov, N., Law, R., et al., 2001. Coesite in Himalayan Eclogite and Implications for Models of India-Asia Collision. *Geology*, 29(5): 435. [https://doi.org/10.1130/0091-7613\(2001\)029<0435:ciheai>2.0.co;2](https://doi.org/10.1130/0091-7613(2001)029<0435:ciheai>2.0.co;2)
- Patiño Douce, A. E., Harris, N. B. W., 1998. Experimental Constraints on Himalayan Anatexis. *Journal of Petrology*, 39(4): 689–710. <https://doi.org/10.1093/petroj/39.4.689>
- Pognante, U., Benna, P., 1993. Metamorphic Zonation, Migmatization, and Leucogranites along the Everest Transect (Eastern Nepal and Tibet): Record of an Exhumation History. *Geological Society, London, Special Publication*, 74 (1): 323–340. <https://doi.org/10.1144/GSL.SP.1993.074.01.22>
- Pognante, U., Lombardo, B., 1989. Metamorphic Evolution of the High Himalayan Crystallines in SE Zaskar, India. *Journal of Metamorphic Geology*, 7 (1): 9–17. <https://doi.org/10.1111/j.1525-1314.1989.tb00571.x>
- Prince, C., Harris, N. B. W., Vance, D., 2001. Fluid-Enhanced Melting during Prograde Metamorphism. *Journal of the Geological Society*, 158(2): 233–241. <https://doi.org/10.1144/jgs.158.2.233>
- Qi, X. X., Zeng, L. S., Meng, X. J., et al., 2008. Zircon SHRIMP U-Pb Dating for Dala Granite in the Tethyan Himalaya and Its Geological Implication. *Acta Petrologica Sinica*, 24(7): 1501–1508 (in Chinese with English abstract).
- Regis, D., Warren, C. J., Mottram, C. M., et al., 2016. Using Monazite and Zircon Petrochronology to Constrain the *P-T-t* Evolution of the Middle Crust in the Bhutan Himalaya. *Journal of Metamorphic Geology*, 34 (6): 617–639. <https://doi.org/10.1111/jmg.12196>
- Regis, D., Warren, C. J., Young, D., et al., 2014. Tectono-Metamorphic Evolution of the Jomolhari Massif: Variations in Timing of Syn-Collisional Metamorphism across Western Bhutan. *Lithos*, 190–191: 449–466. <https://doi.org/10.1016/j.lithos.2014.01.001>
- Rubatto, D., Chakraborty, S., Dasgupta, S., 2013. Timescales of Crustal Melting in the Higher Himalayan Crystallines (Sikkim, Eastern Himalaya) Inferred from Trace Element-Constrained Monazite and Zircon Chronology. *Contributions to Mineralogy and Petrology*, 165 (2): 349–372. <https://doi.org/10.1007/s00410-012-0812-y>
- Sachan, H. K., Kohn, M. J., Saxena, A., et al., 2010. The Malari Leucogranite, Garhwal Himalaya, Northern India: Chemistry, Age, and Tectonic Implications. *Geological Society of America Bulletin*, 122 (11–12): 1865–1876. <https://doi.org/10.1130/b30153.1>
- Sachan, H. K., Mukherjee, B. K., Ogasawara, Y., et al., 2004. Discovery of Coesite from Indus Suture Zone (ISZ), Ladakh, India; Evidence for Deep Subduction. *European Journal of Mineralogy*, 16(2): 235–240. <https://doi.org/10.1127/0935-1221/2004/0016-0235>
- Scaillet, B., France-Lanord, C., Le Fort, P., 1990. Badrinath-Gangotri Plutons (Garhwal, India): Petrological and Geochemical Evidence for Fractionation Processes in a High Himalayan Leucogranite. *Journal of Volcanology and Geothermal Research*, 44 (1–2): 163–188. [https://doi.org/10.1016/0377-0273\(90\)90017-a](https://doi.org/10.1016/0377-0273(90)90017-a)
- Searle, M. P., 1999. Extensional and Compressional Faults in the Everest Lhotse Massif, Khumbu Himalaya, Nepal. *Journal of the Geological Society*, 156(2): 227–240. <https://doi.org/10.1144/gsjgs.156.2.0227>
- Searle, M. P., Godin, L., 2003. The South Tibetan Detachment and the Manaslu Leucogranite: A Structural Reinterpretation and Restoration of the Annapurna-Manaslu Himalaya, Nepal. *The Journal of Geology*, 111(5): 505–523. <https://doi.org/10.1086/376763>
- Smit, M. A., Hacker, B. R., Lee, J., 2014. Tibetan Garnet Records Early Eocene Initiation of Thickening in the Himalaya. *Geology*, 42(7): 591–594. <https://doi.org/10.1130/g35524.1>
- Sorcar, N., Hoppe, U., Dasgupta, S., et al., 2014. High-Temperature Cooling Histories of Migmatites from the High Himalayan Crystallines in Sikkim, India: Rapid Cooling Unrelated to Exhumation? *Contributions to Mineralogy and Petrology*, 167(2): 1–34. <https://doi.org/10.1007/s00410-013-0957-3>
- Streule, M. J., Searle, M. P., Waters, D. J., et al., 2010. Metamorphism, Melting, and Channel Flow in the Greater Himalayan Sequence and Makalu Leucogranite: Constraints from Thermobarometry, Metamorphic Modeling, and U-Pb Geochronology. *Tectonics*, 29 (5): TC5011. <https://doi.org/10.1029/2009tc002533>

- St-Onge, M. R., Rayner, N., Palin, R. M., et al., 2013. Integrated Pressure-Temperature-Time Constraints for the Tso Moriri Dome (Northwest India): Implications for the Burial and Exhumation Path of UHP Units in the Western Himalaya. *Journal of Metamorphic Geology*, 31(5): 469–504. <https://doi.org/10.1111/jmg.12030>
- Tian, Z., Zhang, Z. M., Dong, X., 2016. Metamorphism of High-P Metagreywacke from the Eastern Himalayan Syntaxis: Phase Equilibria and *P-T* Path. *Journal of Metamorphic Geology*, 34(7): 697–718. <https://doi.org/10.1111/jmg.12205>
- Tian, Z. L., Kang, D. Y., Mu, H. C., 2017. Metamorphic *P-T-t* Path of Garnet Amphibolite from the Eastern Himalaya Syntaxis: Phase Equilibria and Zircon Chronology. *Acta Petrologica Sinica*, 33(8): 2467–2478 (in Chinese with English abstract).
- Tobgay, T., McQuarrie, N., Long, S., et al., 2012. The Age and Rate of Displacement along the Main Central Thrust in the Western Bhutan Himalaya. *Earth and Planetary Science Letters*, 319–320: 146–158. <https://doi.org/10.1016/j.epsl.2011.12.005>
- Viskupic, K., Hodges, K. V., 2001. Monazite-Xenotime Thermochronometry: Methodology and an Example from the Nepalese Himalaya. *Contributions to Mineralogy and Petrology*, 141(2): 233–247. <https://doi.org/10.1007/s004100100239>
- Viskupic, K., Hodges, K. V., Bowring, S. A., 2005. Timescales of Melt Generation and the Thermal Evolution of the Himalayan Metamorphic Core, Everest Region, Eastern Nepal. *Contributions to Mineralogy and Petrology*, 149(1): 1–21. <https://doi.org/10.1007/s00410-004-0628-5>
- Visonà, D., Carosi, R., Montomoli, C., et al., 2012. Miocene Andalusite Leucogranite in Central-East Himalaya (Everest-Masang Kang Area): Low-Pressure Melting during Heating. *Lithos*, 144–145: 194–208. <https://doi.org/10.1016/j.lithos.2012.04.012>
- Wang, J. M., Rubatto, D., Zhang, J. J., 2015a. Timing of Partial Melting and Cooling across the Greater Himalayan Crystalline Complex (Nyalam, Central Himalaya): In-Sequence Thrusting and Its Implications. *Journal of Petrology*, 56(9): 1677–1702. <https://doi.org/10.1093/petrology/egv050>
- Wang, J. M., Wu, F. Y., Rubatto, D., et al., 2017b. Monazite Behaviour during Isothermal Decompression in Pelitic Granulites: A Case Study from Dinggye, Tibetan Himalaya. *Contributions to Mineralogy and Petrology*, 172(10): 1–30. <https://doi.org/10.1007/s00410-017-1400-y>
- Wang, J. M., Zhang, J. J., Liu, K., et al., 2016. Spatial and Temporal Evolution of Tectonometamorphic Discontinuities in the Central Himalaya: Constraints from *P-T* Paths and Geochronology. *Tectonophysics*, 679: 41–60. <https://doi.org/10.1016/j.tecto.2016.04.035>
- Wang, J. M., Zhang, J. J., Wang, X. X., 2013. Structural Kinematics, Metamorphic *P-T* Profiles and Zircon Geochronology across the Greater Himalayan Crystalline Complex in South-Central Tibet: Implication for a Revised Channel Flow. *Journal of Metamorphic Geology*, 31(6): 607–628. <https://doi.org/10.1111/jmg.12036>
- Wang, J. M., Zhang, J. J., Wei, C. J., et al., 2015b. Characterising the Metamorphic Discontinuity across the Main Central Thrust Zone of Eastern-Central Nepal. *Journal of Asian Earth Sciences*, 101: 83–100. <https://doi.org/10.1016/j.jseaes.2015.01.027>
- Wang, Y. H., Zhang, L. F., Zhang, J. J., et al., 2017a. The Youngest Eclogite in Central Himalaya: *P-T* Path, U-Pb Zircon Age and Its Tectonic Implication. *Gondwana Research*, 41: 188–206. <https://doi.org/10.1016/j.gr.2015.10.013>
- Warren, C. J., Grujic, D., Kellett, D. A., et al., 2011. Probing the Depths of the India-Asia Collision: U-Th-Pb Monazite Chronology of Granulites from NW Bhutan. *Tectonics*, 30(2): TC2004. <https://doi.org/10.1029/2010tc002738>
- Wei, C. J., Guan, X., Dong, J., 2017. HT-UHP Metamorphism of Metabasites and the Petrogenesis of TTGs. *Acta Petrologica Sinica*, 33(5): 1381–1404 (in Chinese with English abstract).
- Weinberg, R. F., 2016. Himalayan Leucogranites and Migmatites: Nature, Timing and Duration of Anatexis. *Journal of Metamorphic Geology*, 34(8): 821–843. <https://doi.org/10.1111/jmg.12204>
- Wu, F. Y., Liu, Z. C., Liu, X. C., et al., 2015. Himalayan Leucogranite: Petrogenesis and Implications to Orogenesis and Plateau Uplift. *Acta Petrologica Sinica*, 31(1): 1–36 (in Chinese with English abstract).
- Xiang, H., Zhang, Z. M., Dong, X., et al., 2013. High-Pressure Metamorphism and Anatexis during the Subduction of Indian Continent: Phase Equilibria Modeling of the Namche Barwa Complex, Eastern Himalayan Syntaxis. *Acta Petrologica Sinica*, 29(11): 3792–3802 (in Chinese with English abstract).
- Yin, A., Harrison, T. M., 2000. Geologic Evolution of the Himalayan-Tibetan Orogen. *Annual Review of Earth and Planetary Sciences*, 28(1): 211–280. <https://doi.org/10.1146/annurev.earth.28.1.211>
- Zeiger, K., Gordon, S. M., Long, S. P., et al., 2015. Timing and Conditions of Metamorphism and Melt Crystallization

- in Greater Himalayan Rocks, Eastern and Central Bhutan; Insight from U-Pb Zircon and Monazite Geochronology and Trace-Element Analyses. *Contributions to Mineralogy and Petrology*, 169 (5): 47. <https://doi.org/10.1007/s00410-015-1143-6>
- Zeng, L. S., Gao, L. E., 2017. Cenozoic Crustal Anatexis and the Leucogranites in the Himalayan Collisional Orogenic Belt. *Acta Petrologica Sinica*, 33(5): 1420–1444 (in Chinese with English abstract).
- Zeng, L. S., Gao, L. E., Dong, C. Y., et al., 2012. High-Pressure Melting of Metapelite and the Formation of Ca-Rich Granitic Melts in the Namche Barwa Massif, Southern Tibet. *Gondwana Research*, 21(1): 138–151. <https://doi.org/10.1016/j.gr.2011.07.023>
- Zeng, L. S., Gao, L. E., Tang, S. H., et al., 2015. Eocene Magmatism in the Tethyan Himalaya, Southern Tibet. *Geological Society, London, Special Publications*, 412(1): 287–316. <https://doi.org/10.1144/SP412.8>
- Zeng, L. S., Gao, L. E., Xie, K. J., et al., 2011. Mid-Eocene High Sr/Y Granites in the Northern Himalayan Gneiss Domes: Melting Thickened Lower Continental Crust. *Earth and Planetary Science Letters*, 303(3–4): 251–266. <https://doi.org/10.1016/j.epsl.2011.01.005>
- Zhang, H. F., Harris, N. B. W., Parrish, R., et al., 2004. Causes and Consequences of Protracted Melting of the Mid-Crust Exposed in the North Himalayan Antiform. *Earth and Planetary Science Letters*, 228(1–2): 195–212. <https://doi.org/10.1016/j.epsl.2004.09.031>
- Zhang, J. J., Santosh, M., Wang, X. X., et al., 2012a. Tectonics of the Northern Himalaya since the India-Asia Collision. *Gondwana Research*, 21(4): 939–960. <https://doi.org/10.1016/j.gr.2011.11.004>
- Zhang, Z. M., Dong, X., Ding, H. X., et al., 2017. Metamorphism and Partial Melting of the Himalayan Orogen. *Acta Petrologica Sinica*, 33(8): 2313–2341 (in Chinese with English abstract).
- Zhang, Z. M., Dong, X., Santosh, M., et al., 2012b. Petrology and Geochronology of the Namche Barwa Complex in the Eastern Himalayan Syntaxis, Tibet: Constraints on the Origin and Evolution of the North-Eastern Margin of the Indian Craton. *Gondwana Research*, 21(1): 123–137. <https://doi.org/10.1016/j.gr.2011.02.002>
- Zhang, Z. M., Xiang, H., Ding, H. X., et al., 2017a. Miocene Orbicular Diorite in East-Central Himalaya: Anatexis, Melt Mixing, and Fractional Crystallization of the Greater Himalayan Sequence. *Geological Society of America Bulletin*, 129(7–8): 869–885. <https://doi.org/10.1130/b31586.1>
- Zhang, Z. M., Xiang, H., Dong, X., et al., 2015. Long-Lived High-Temperature Granulite-Facies Metamorphism in the Eastern Himalayan Orogen, South Tibet. *Lithos*, 212–215: 1–15. <https://doi.org/10.1016/j.lithos.2014.10.009>
- Zhang, Z. M., Xiang, H., Dong, X., et al., 2017b. Oligocene HP Metamorphism and Anatexis of the Higher Himalayan Crystalline Sequence in Yadong Region, East-Central Himalaya. *Gondwana Research*, 41: 173–187. <https://doi.org/10.1016/j.gr.2015.03.002>
- Zhang, Z. M., Zhao, G. C., Santosh, M., et al., 2010. Two Stages of Granulite Facies Metamorphism in the Eastern Himalayan Syntaxis, South Tibet: Petrology, Zircon Geochronology and Implications for the Subduction of Neo-Tethys and the Indian Continent beneath Asia. *Journal of Metamorphic Geology*, 28(7): 719–733. <https://doi.org/10.1111/j.1525-1314.2010.00885.x>

附中文参考文献

- 刘凤麟, 张立飞, 2014. 喜马拉雅东构造结高压麻粒岩 PT 轨迹, 锆石 U-Pb 定年及其地质意义. *岩石学报*, 30(10): 2808–2820.
- 戚学祥, 曾令森, 孟祥金, 等, 2008. 提提斯喜马拉雅打拉花岗岩的锆石 SHRIMP U-Pb 定年及其地质意义. *岩石学报*, 24(7): 1501–1508.
- 田作林, 康东艳, 穆虹辰, 2017. 东喜马拉雅构造结石榴角闪岩变质作用 $P-T-t$ 轨迹: 相平衡模拟与锆石年代学. *岩石学报*, 33(8): 2467–2478.
- 魏春景, 关晓, 董杰, 2017. 基性岩高温—超高压变质作用与 TTG 质岩成因. *岩石学报*, 33(5): 1381–1404.
- 吴福元, 刘志超, 刘小驰, 等, 2015. 喜马拉雅淡色花岗岩. *岩石学报*, 31(1): 1–36.
- 向华, 张泽明, 董昕, 等, 2013. 印度大陆俯冲过程中的高压变质与深熔作用: 东喜马拉雅构造结南迦巴瓦杂岩的相平衡模拟研究. *岩石学报*, 29(11): 3792–3802.
- 曾令森, 高利娥, 2017. 喜马拉雅碰撞造山带新生代地壳深熔作用与淡色花岗岩. *岩石学报*, 33(5): 1420–1444.
- 张泽明, 董昕, 丁慧霞, 等, 2017. 喜马拉雅造山带的变质作用与部分熔融. *岩石学报*, 33(8): 2313–2341.